

Supplement of Nat. Hazards Earth Syst. Sci., 20, 1573–1593, 2020
<https://doi.org/10.5194/nhess-20-1573-2020-supplement>
© Author(s) 2020. This work is distributed under
the Creative Commons Attribution 4.0 License.



Supplement of

Induced seismicity risk analysis of the hydraulic stimulation of a geothermal well on Geldinganes, Iceland

Marco Broccardo et al.

Correspondence to: Marco Broccardo (bromarco@ethz.ch)

The copyright of individual parts of the supplement might differ from the CC BY 4.0 License.

Supplements

S1 GMPEs GMICE and Scenario based intensity

In this Supplementary material, we first show the trellis plots of the GMPE Figure S1 and of the GMPE&GMICE combination, Figure S2. The GMICE coefficients are reported in Table S1.

5

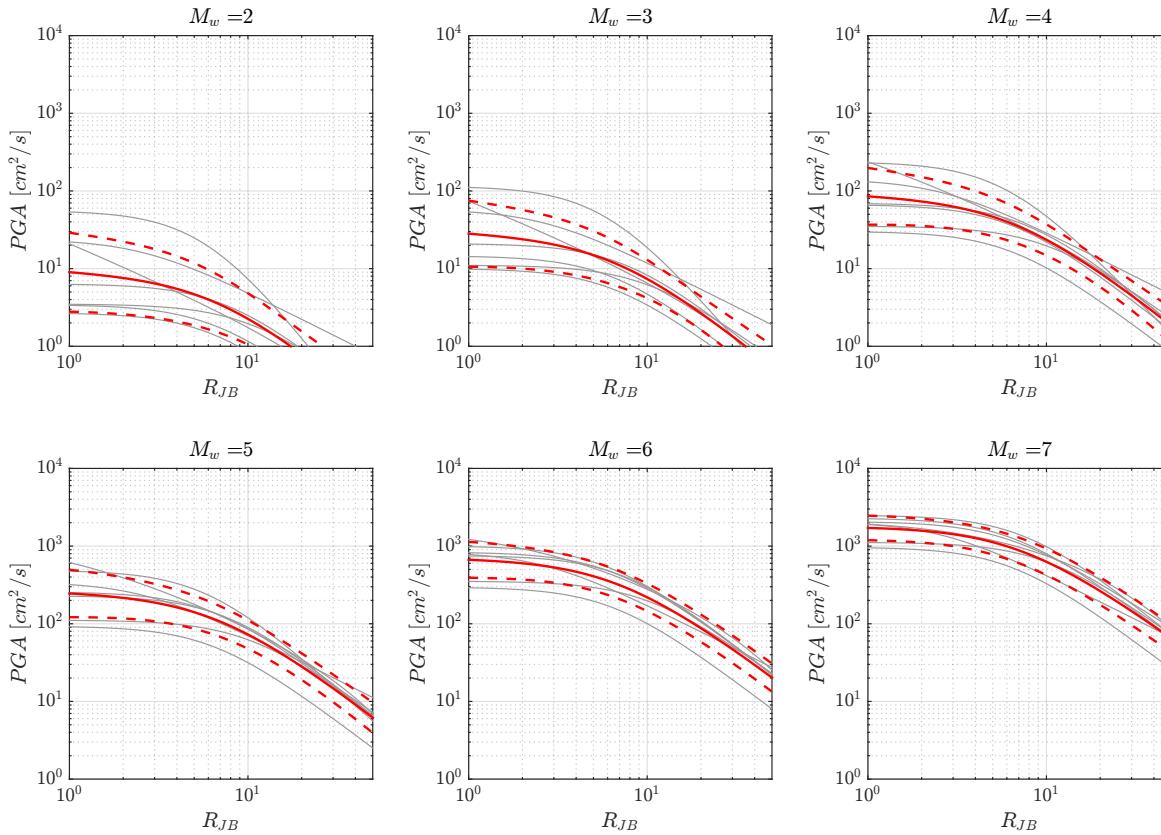
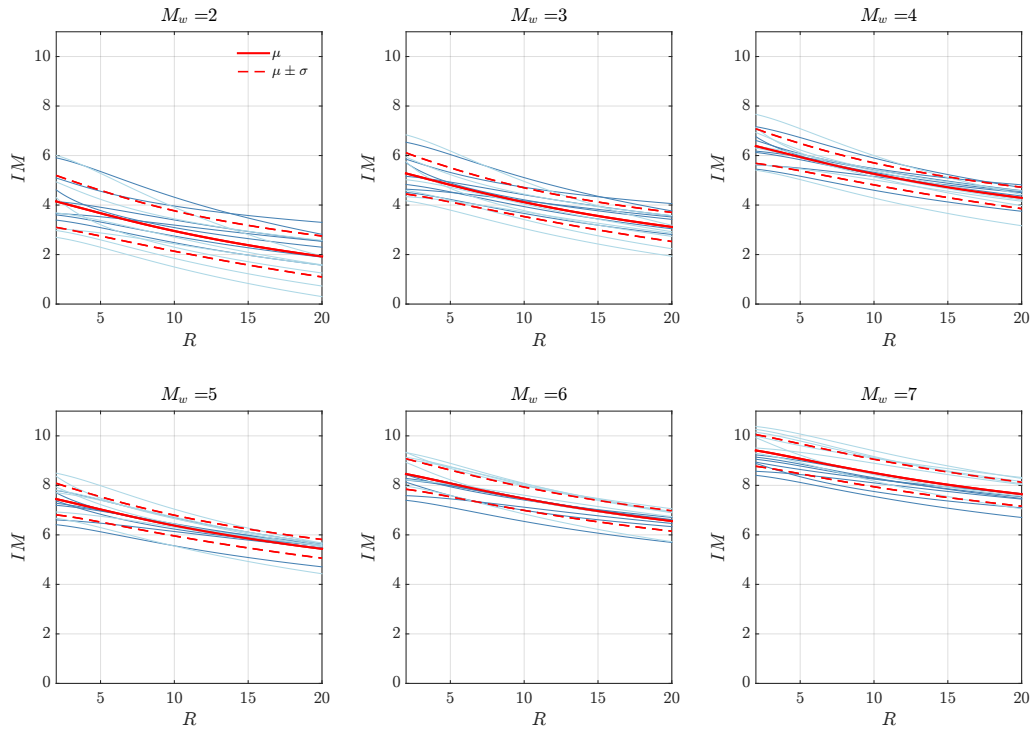


Figure S1. Trellis Plots for the selected GMPEs models. Following the same representation of Rupakhety and Sigjörnsson (2009), solid red lines are the epistemic mean and the dash lines the epistemic mean plus minus the epistemic standard deviation (in log scale).



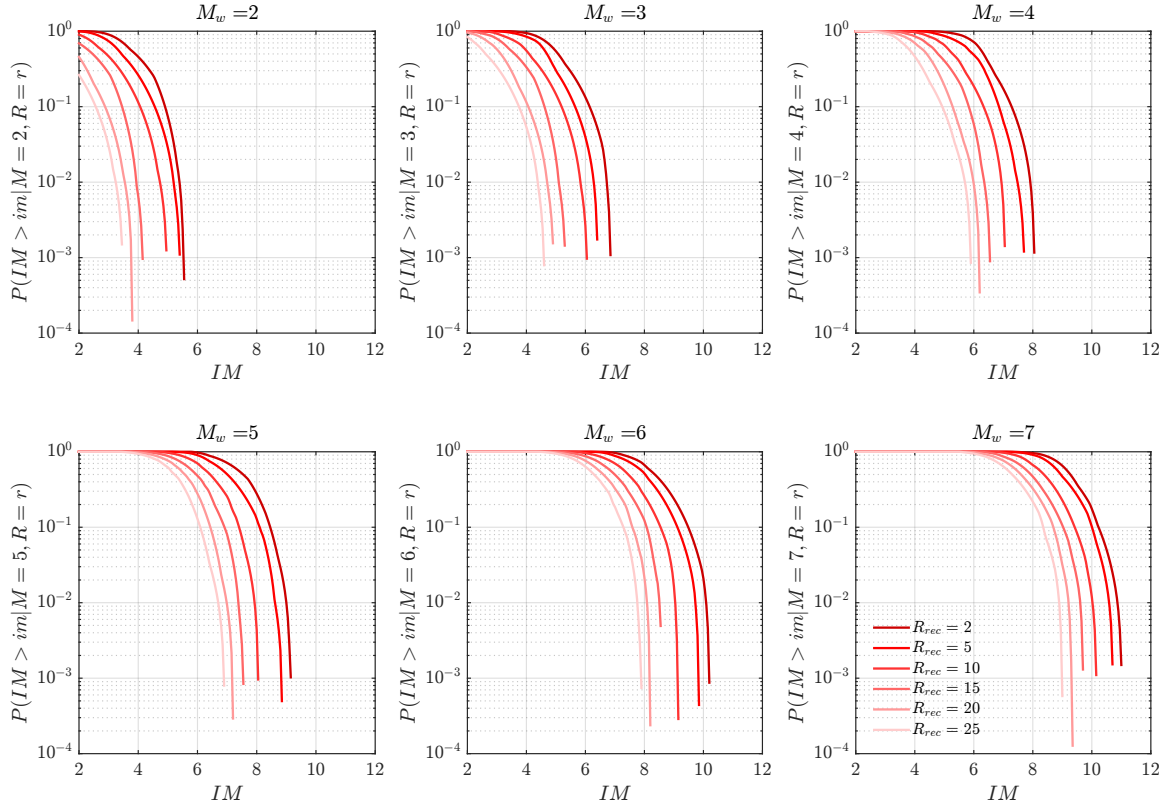
10

Figure S2 GMICE model. Solid red lines are the epistemic mean and the dash lines the epistemic mean plus minus the epistemic standard deviation.

Table S1: GMICE parameter list

| | $\mu_{IM}(PGA)$ | σ_{GMICE} | | σ_{GMPE} | a | σ_{TOT} |
|----------------------------------------------|------------------------------|------------------|--------|-----------------|----------------|----------------|
| Faccioli and Cauzzi (2006) Units: [m/s] | $1.96 \log_{10}(PGA) + 6.54$ | 0.89 | 1-AB10 | 0.175 | 1.96 | 0.954 |
| | | | 2-CF08 | 0.176 | 1.96 | 0.955 |
| | | | 3-Zh06 | 0.391 | $1.96/\ln(10)$ | 0.950 |
| | | | 4-Am05 | 0.175 | 1.96 | 0.954 |
| | | | 5-DT07 | 0.177 | 1.96 | 0.955 |
| | | | 6-GK02 | 0.403 | $1.96/\ln(10)$ | 0.954 |
| | | | 7-RS09 | 0.287 | 1.96 | 1.053 |
| Faenza and Michelini (2010) Units: [cm/s] | $2.58 \log_{10}(PGA) + 1.68$ | 0.35 | 1-AB10 | 0.175 | 2.58 | 0.571 |
| | | | 2-CF08 | 0.176 | 2.58 | 0.573 |
| | | | 3-Zh06 | 0.391 | $2.58/\ln(10)$ | 0.560 |
| | | | 4-Am05 | 0.175 | 2.58 | 0.571 |
| | | | 5-DT07 | 0.177 | 2.58 | 0.575 |
| | | | 6-GK02 | 0.403 | $2.58/\ln(10)$ | 0.571 |
| | | | 7-RS09 | 0.287 | 2.58 | 0.819 |

Given the very large epistemic uncertainty governing the parameter a_{fb} and b of the seismogenic source model, here we propose a conditional probability distribution of PGA and IM : i.e., $P(PGA > pga|M = m, r)$ (also known as scenario based distribution). Figure S3 shows the scenario-based distributions for both PGA and IM .



20

Figure S3 Collection of epistemic medians of $P(IM > im|M = m, R = r)$ for different Magnitude and site to source distances

S2 Exposure, population and assets

The exposed area to the introduced anthropogenic hazard is defined by the building stock within approximately 20 km from the injection point. The region is identified with the so-called Höfuðborgarsvæðið (i.e., the capital region, which includes the capital Reykjavík and six municipalities). This is the largest and densest urban agglomeration in the country with a population of 229,000, which corresponds to circa 65% of the total Icelandic population.

For this study, detailed and precise information of the Reykjavik building stock and population exposed is not readily available and hence not used. Therefore, this description is limited to a macro analysis based on the work of Bessason and

30 Bjarnason (2016), the Icelandic Property Registry, and the European Seismic Risk service. Based on the Icelandic Property
Registry and on Bessason and Bjarnason (2016), it is possible to categorize the building stock by the class of buildings.
According to Bessason and Bjarnason (2016), the vast majority of residential buildings (reinforced concrete, timber and pumice
block buildings) have shear walls as a lateral structural system against seismic forces. Buildings made of hollow pumice
35 represent a small percentage and can be considered according to Bessason and Bjarnason (2016) as masonry buildings. No
information is available at the present time on soil conditions at construction sites, which is assumed to be in firm soil condition.
We finally highlight that these evaluations are a first-order estimate only. Given the current lack of a detailed exposure model,
we do not include in the present study any aggregate monetary loss analysis.

In addition, according to the European Seismic Risk service, the residential building stock of Iceland is composed of
circa 70,000 buildings with a total of 68,000 million Euro of replacement costs. In a first-order inference of the number of
40 residential buildings, we can estimate that there are circa 55-65% of the total amount, a percentage a bit lower than the
population proportion. This assumes that in urban areas, the number of persons per building is higher. Given that, a crude
estimate of the number of residential buildings in the considered area is given by a range of 38,500-45,500 units for a total
replacement cost of [37,400-44,200] millions of euro.

We highlight that these evaluations are a crude first-order estimate only. Given the current lack of a detailed exposure
45 model, we do not include in the present study an aggregate monetary loss analysis (since it will introduce an additional level
of deep uncertainty). However, we introduced a low damage threshold risk metric to measure and prevent the likelihood of
large damage in the building stock.

50

S3 Scenario Based *IR*, and *DR*

In this section, we first present the scenario *IR* for different magnitudes, locations and building typologies. The scenarios are
derived by using the mean of the GMICE and converted into *IR* by using the vulnerability model (Lagomarsino and
Giovinazzi, 2006, and modified by Mignan et al. 2015, Figure S4, Table S2) and the conditional probability of fatalities for a
55 given damage grade (Galanis et al. 2018, Hazus MH MR3, 2003). Figure S5 shows the *IR* scenario-based calculations. We
can conclude that for a magnitude lower than 4 the $IR = q_{IR,5} \leq 10^{-6}$ is satisfied for all the building classes.

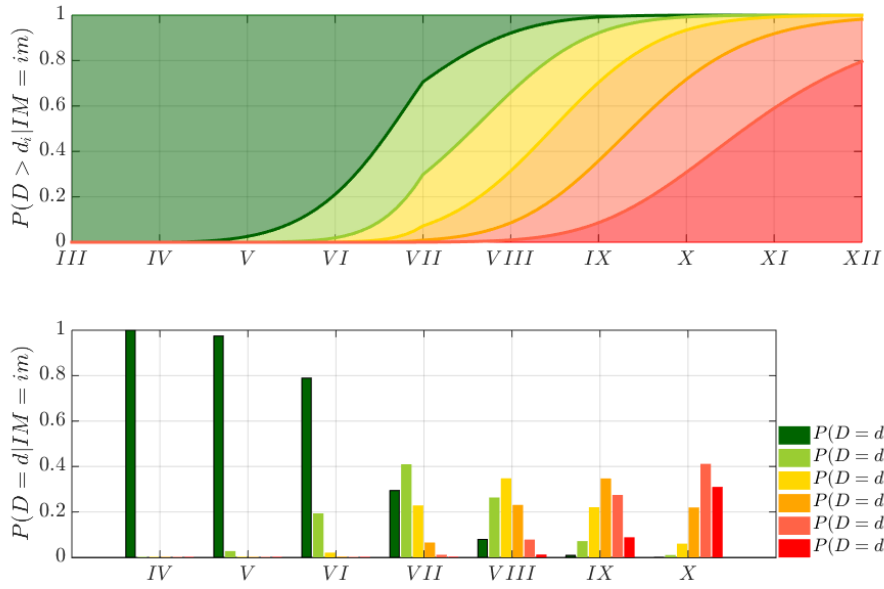


Figure S4 Top subplot: fragility functions, $P(D > d_k | IM = im)$, bottom subplot: probability mass function $p_D(d_k)$ for different level of intensity. The discontinuity at $im = VII$ is introduced by Mignan et al. (2015).

60

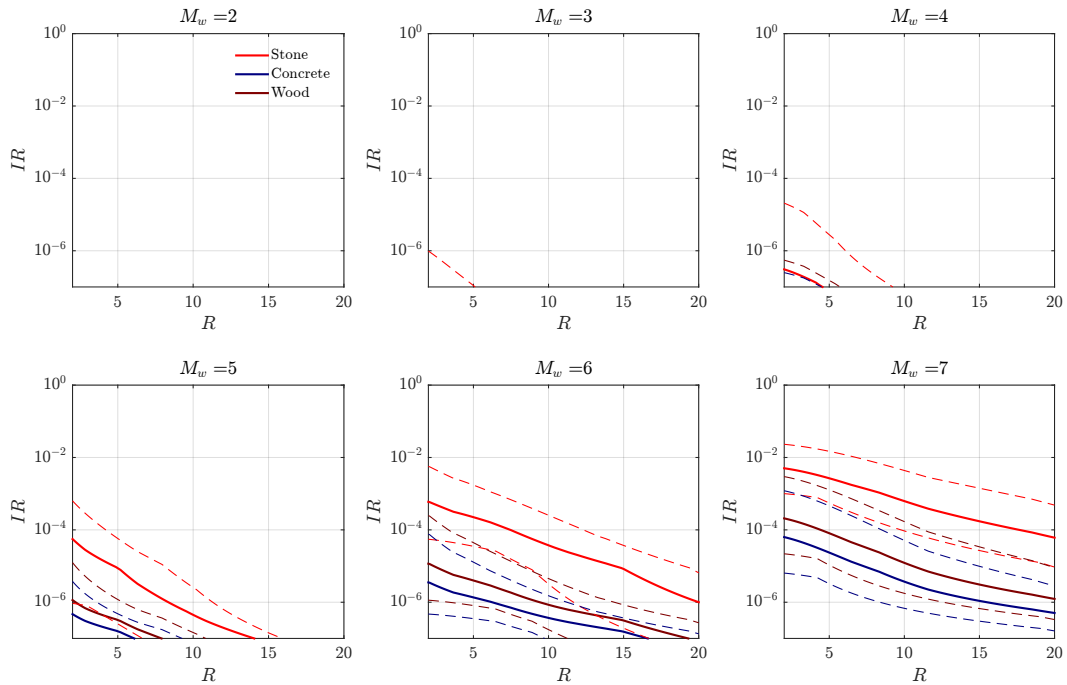


Figure S5. Individual Risk for different magnitude, distance and typology of buildings.

Further, we present damage-based scenarios derived by using the mean of the GMICE converted into DR by using the local fragility functions proposed by Besson, B. and Bjarnason, 2016, reproduced in Figure S6.

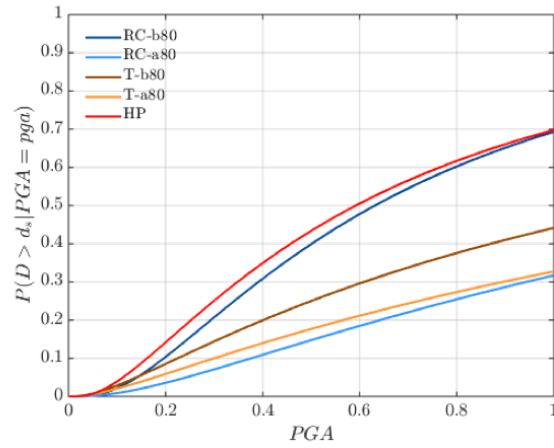


Figure S6 Fragility function for low damage estimation

Figure S7 shows the damage scenario for a magnitude 3 and 4, which represent the scenario limit for observing $DR \leq 10^{-2}$.

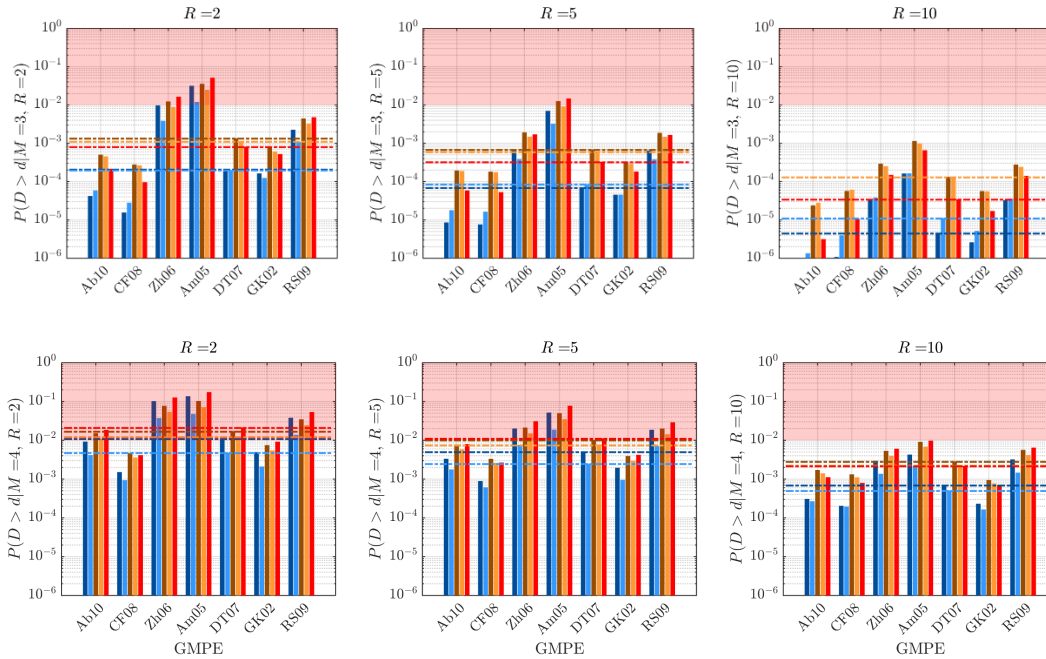


Figure S7. Scenario-based Damage Risk for magnitude 3 (first 3 subplots) or 4 (second 3 subplots). Dashed lines represent the median for each building class.

Table S2 Vulnerability index per building class. V^0 , V^+ , V^- & V^{--} , V^{++} values are based on Mignan et al. (2015). Bolt fonts indicate the selected model.

| Building class | Class description | V^{--} | V^- | V^0 | V^+ | V^{++} |
|----------------|-------------------|----------|-------|-------|-------|----------|
|----------------|-------------------|----------|-------|-------|-------|----------|

| | | | | | | | |
|---------------------|-------------------------------------|----------------------------------------|--------|--------------|--------------|-------|-------|
| Masonry (M) | M1 | Simple stone with timber slabs | 0.460 | 0.650 | 0.740 | 0.830 | 1.020 |
| | M2 | Massive stone with timber slabs | 0.300 | 0.490 | 0.616 | 0.793 | 0.860 |
| | M3 | Brick with concrete slabs | 0.300 | 0.490 | 0.616 | 0.793 | 0.860 |
| | M4 | Simple stone with hollow-core slabs | 0.420 | 0.610 | 0.700 | 0.790 | 0.900 |
| | M5 | Brick with hollow-core slabs | 0.320 | 0.500 | 0.650 | 0.800 | 0.870 |
| | M6 | Massive stone with hollow-core slabs | 0.320 | 0.500 | 0.650 | 0.800 | 0.870 |
| | M7 | Brick with timber slabs | 0.460 | 0.650 | 0.740 | 0.830 | 1.020 |
| Reinforced concrete | RC | | | | | | |
| | 1 | Concrete moment frames | 0.140 | 0.207 | 0.442 | 0.640 | 0.860 |
| | RC | | | | | | |
| | 2 | Concrete shear walls | 0.140 | 0.210 | 0.386 | 0.510 | 0.700 |
| | RC | | | | | | |
| | 3 | Concrete walls and brick masonry walls | 0.150 | 0.220 | 0.400 | 0.520 | 0.710 |
| RC | | | | | | | |
| 4 | Hennebique system | 0.250 | 0.300 | 0.500 | 0.700 | 0.850 | |
| RC | | | | | | | |
| 4 | Concrete moment frames with infills | 0.150 | 0.220 | 0.402 | 0.520 | 0.710 | |
| Steel | S1 | Steel Structures (moment & brace F) | -0.020 | 0.170 | 0.325 | 0.480 | 0.700 |
| | S2 | Old steel structures | 0.150 | 0.220 | 0.400 | 0.520 | 0.710 |
| Wood | W1 | Timber structures | 0.140 | 0.207 | 0.447 | 0.640 | 0.860 |
| | W2 | Half-timbered structures | 0.170 | 0.240 | 0.480 | 0.670 | 0.890 |

S4 Sensitivity analysis details

In this section, we present the details of the modified version of the Morris method for sensitivity analysis. The modified version is a global sensitivity measure which accounts for all possible base rate model. To obtain a global sensitivity measure, we first
80 define the local sensitivity measure of the parameter i with respect to the model base j as

$$d_i(j) = \frac{\max[\text{QoI}_i(j)] - \min[\text{QoI}_i(j)]}{\Delta}, \quad (\text{S1})$$

where $\max(\text{QoI}_i(j))$ and $\min(\text{QoI}_i(j))$ are the maximum positive and negative swings of the selected QoI obtained by holding all the parameter different from i fixed to their base value j . Moreover, $\Delta = \max(\text{QoI}) - \min(\text{QoI})$ is the global maximum swing of the QoI (which is by definition independent on i or j). Then, we define two global sensitivity measures as

85

$$\mu_{d_i} = \frac{1}{J} \sum_{j=1}^J d_i(j), \quad (\text{S2})$$

$$\bar{d}_i = \max[d_i(j)]. \quad (\text{S3})$$

In particular, the sensitivity measure μ_{d_i} aims to provide an average relative contribution of the parameter i over all possible base models. On the other hand, the sensitivity measure \bar{d}_i aims to describe the maximum contribution of the parameter i over all possible base models. Observe that $0 \leq \mu_{d_i} \leq 1$ and $0 \leq \bar{d}_i \leq 1$ and the sum over i for both, in general, is not equal to 1
 90 (obviously one can normalize the output if this is a desired property). Therefore, the following sensitivity method shall be used only to rank the input uncertainties and to understand their relative contribution and not the absolute contribution.

In this study IR and DR , range from medium-low probability values to very low probability values, with values that go from 10^{-2} (DR) up to 10^{-14} (IR). Therefore, to avoid the dominant contribution of the branches with higher probability content, we performed a log transformation. It follows that the two QoIs are: $\log(IR)$ and $\log(DR)$. In the following we report the results
 95 for \bar{d}_i (while μ_{d_i} are reported in the main text). Figures S8 and S9 show the same trend observed for μ_{d_i} with the rate model dominant for both datasets and with a relatively larger contribution of the dataset based on Table 3.1.

100

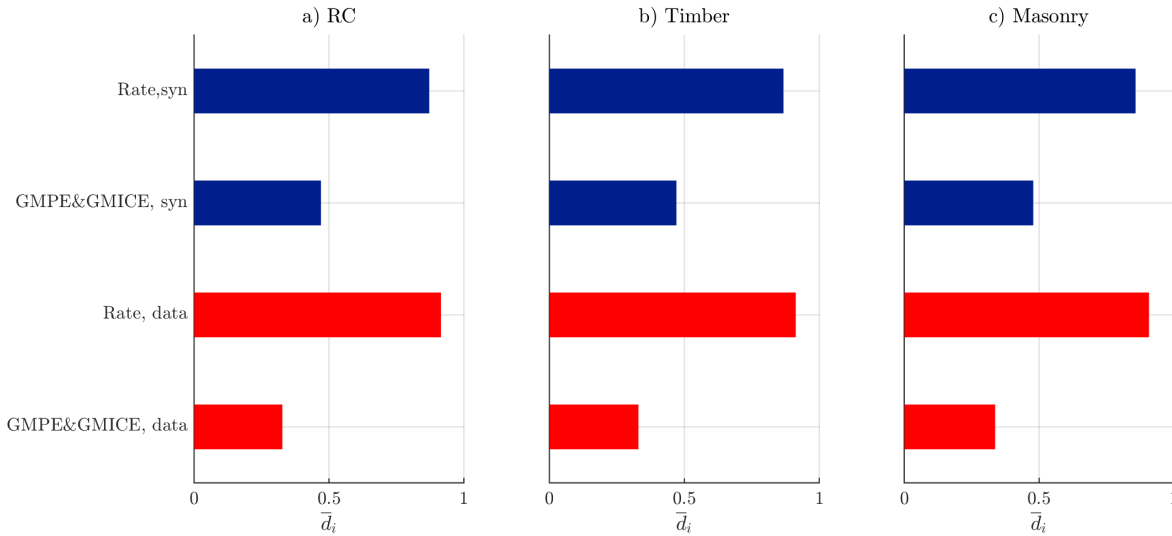
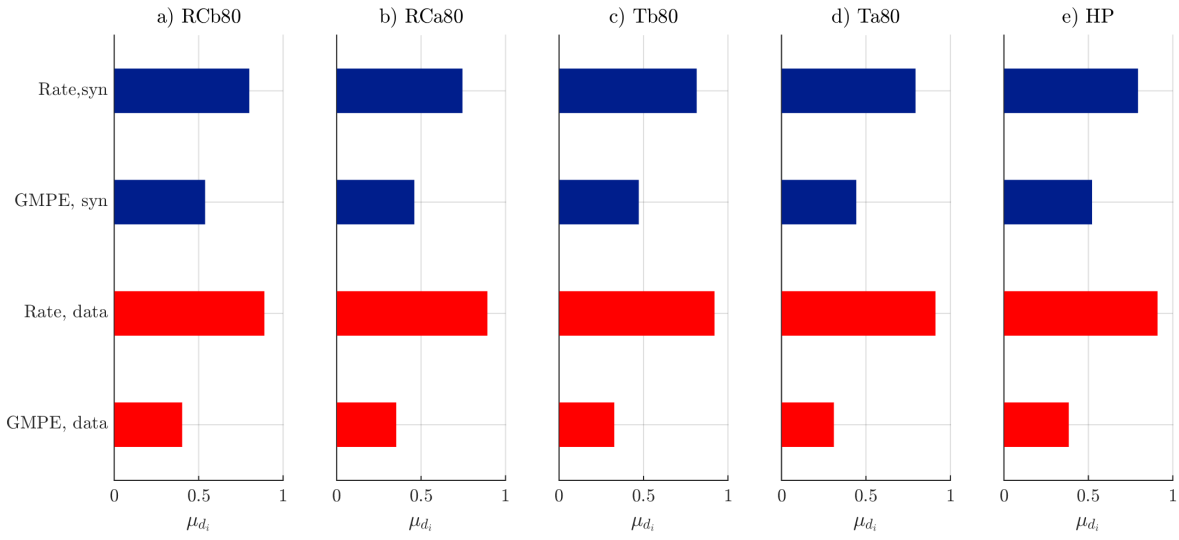


Figure S8. Sensitivity analysis of IR (observe that the QoI is $\log IR$) based on the sensitivity measure \bar{d}_i for each building class



105

Figure S9. Sensitivity analysis of DR (observe that the QoI is $\log DR$) based on the sensitivity measure \bar{d}_i for each building class